Talanta 96 (2012) 132–139

Contents lists available at SciVerse ScienceDirect

Talanta

journal homepage: www.elsevier.com/locate/talanta

Performance of an organic photodiode as an optical detector and its application to fluorometric flow-immunoassay for IgA

Mayo Miyake[a], Hizuru Nakajima[b,**], Akihide Hemmi[c], Masayuki Yahiro[d], Chihaya Adachi[a,e], Nobuaki Soh[f], Ryoichi Ishimatsu[a], Koji Nakano[a], Katsumi Uchiyama[b], Toshihiko Imato[a,*]

[a] Department of Applied Chemistry, Graduate School of Engineering, Kyushu University, 744 Motooka, Nishi-ku, Fukuoka 819-0395, Japan
[b] Department of Applied Chemistry, Graduate School of Urban Environmental Sciences, Tokyo Metropolitan University, 1-1 Minamiohsawa, Hachioji, Tokyo 192-0397, Japan
[c] Mebius Advanced Technology Ltd., 3-31-6-107 Nishiogi-kita, Suginami-ku, Tokyo 167-0042, Japan
[d] Institute of System, Information Technologies and Nanotechnologies, 2-1-22 Momochihama, Swawara-ku, Fukuoka 814-0001, Japan
[e] Center for Organic Photonics and Electronics Research, Kyushu University, 744 Motooka, Nishi-ku, Fukuoka 819-0395, Japan
[f] Faculty of Agriculture, Saga University, 1 Honjo-Machi, Saga 840-8502, Japan

ARTICLE INFO

Article history:
Available online 10 February 2012

Keywords:
Organic thin film photodiode
Immunoassay
Fluorometric detection

ABSTRACT

The performance of an organic thin film photodiode (OPD), fabricated from a hetero-junction comprised of two layers of C_{60} and a phthalocyanine-Cu(II) complex was evaluated by detecting the chemiluminescence generated from the reaction of luminol with horseradish peroxidase in the presence of H_2O_2, and the fluorescence from resorufin, as an optical detector. The photocurrent of the OPD was linear with respect to the power of light from a commercial LED. The sensitivity of the OPD was sufficient for detecting chemiluminescence with a power 0.1 μW/cm^2. The OPD was successfully used in a flow-immunoassay for IgA, a marker of human stress, in which a sandwich immunoassay was carried out on the microchip and the fluorescence from resorufin, produced by the enzymatic reaction, was detected. The detection limits for resorufin and IgA were 5.0 μM and 16 ng/mL, respectively. The photosensitivity of the OPD remained relatively constant for a minimum of one year.

1. Introduction

One of trends in analytical chemistry involves the downsizing of conventional analytical systems, such as the micro-total analysis system, referred to as μ-TAS, the lab on a chip and related systems [1–4]. This trend is consistent with the current interest in green chemistry and sustainable chemistry through zero-emissions, energy savings and achieving an environmentally friendly eco-system [5]. In such systems, the sample size can be reduced to volumes in the sub-micro liter range and the consumption of reagents can be correspondingly reduced, thus creating less regent waste. The reaction time can be substantially reduced, due to the short diffusion length and increase in mass transfer. Because of these advantages, numerous studies have been reported dealing with the integration of microchips with separation, reactions, detection for liquid–liquid extraction analysis [6], electrophoretic analysis [7], immunoassay [8], and column chromatography [9]. Contrary to the advantages, the small sample volume in a very thin detection area requires detection techniques that are highly sensitive. An electrochemical detector, such as an ion-selective electrode and a voltammetric detector can be used as a detector in such a microchip [10]. Successful results have been obtained for several analytes based on electrochemical detection, which can be attributed to the fact that an electrochemical detector can be reduced to a suitable size without any loss of the sensitivity. An optical detector such as a thermal lens spectrophotometer [11], a laser-induced fluorescence detector [12] and a chemiluminescence detector [13] based on a photon-multiplier tube (PMT) have also been widely used in conjunction with microchips. One of the advantages of the use of a laser as a light source for a microchip is that the light beam is inherently small and can be readily focused on the small detection area of the microchip. However, such an optical system requires a relatively expensive and large laser, a PMT and a microscope in spite of the small size of the microchip.

The μ-TAS and the lab on a chip would be expected to be used for the on-site monitoring of environmental pollutants, and for point-of-care clinical diagnosis, etc. due to the small size of the microchip, provided that the optical detection system could be down-sized. The progress and adoption of the fabrication technology for organic light emitting diodes (OLEDs) and organic thin film photodiodes (OPDs), has resulted in several papers on application of OLEDs and OPDs to microfludics for optical detection systems

* Corresponding author. Tel.: +81 92 802 2889; fax: +81 92 802 2889.
** Corresponding author. Tel.: +81 42 677 2836; fax: +81 42 677 2836.
E-mail addresses: nakajima-hizuru@tmu.ac.jp (H. Nakajima), imato@cstf.kyushu-u.ac.jp (T. Imato).

0039-9140/$ – see front matter © 2012 Elsevier B.V. All rights reserved.
doi:10.1016/j.talanta.2012.02.006

[14–20]. For example, Edel et al. [14], have reported electrophoretic separation and fluorescence detection of fluorescein and caroxyfluorescein by using a polymer based light emitting diode fabricated with poly(3,4-ethylenedioxythiophen/polystyrene sulfonate/polyfluorene structure as a light source and a conventional optical fiber detector. They obtained a detection limit of 1 μM for both fluorescent dies. Yao et al. have developed a microfluidic device for fluorescence detection of fluorescent dyes, such as rhodamine 6G and Alexa 535 by using a green OLED fabricated from NPB/Alq_3 as an excitation light source. They applied their device to electrophoretic separation bovine serum albumin conjugates of the fluorescent dye [15]. Shin et al. [16] and Kim et al. [17] have reported a fluorescence detection system composed with an OLED fabricated from α-NPD/Alq_3 and a p-i-n diode for the determination of rhodamine 6G and tetramethyl rhodamine and lower detection limit of 1 μM for rhodamine 6G and 10 μM for tetramethyl rhodamine were obtained. Hofmann et al. [18], and Wang et al. [19] have developed a chemiluminescence detection system for H_2O_2 and antioxidants (α-tocopherol, β-carotene and quercetin), respectively by using an OPD fabricated with a heterojunction of a C_{60}/phthalocyanine-Cu(II) (PcCu(II)) complex and an OPD fabricated with a heterojunction of a P3HT/PCBM. They obtained a detection limit of 1 mM for H_2O_2 and 2–50 mM for antioxidants. Pais et al. [20], have developed an integrated fluorescence detection system with an OLED fabricated by PcCu(II)/C_{60} and an OPD fabricated by NPB/Alq_3 on a microfluidic. They measured rhodamine 6G and fluoreceine and obtained the detection limit of 100 nM for rhodamine 6G and 10 μM for fluoresceine, respectively. The most sophisticated artifice is that they used a pair of a polarizer just in front of the OPD and the OLED with perpendicular configuration (crossed Nicols condition) in order to minimize the interference of the light source from the OLED to the fluorescence detection by the OPD. However, a relatively high background current was observed and the photocurrent was proportional to logarithmic concentration of fluorescein and rhodamine 6G, which indicates the sensitivity may be lower than that obtained by Kim et al. [17], where a p–i–n diode was used as a detector.

Research on the development of optical systems for microfluidics using OLEDs and OPDs is just at the initial stage, and the further progress would be expected as a result of the interdisciplinary efforts of analytical chemists and electro and mechanical engineers. The goal of this study is to develop a fluorometric immunoassay system on a microfluidic microchip by integrating an OPD and an OLED. At the initial stage of our objective, we applied an OPD as an optical detector to a fluorometric immunoassay on a microfluidic microchip.

In this paper, the performance of the OPD fabricated from a conventional hetero-junction of C_{60} and a PcCu(II) complex, which is usually used as a solar cell, was examined by the detection of chemiluminescence light from a luminol reaction and fluorescence light from resorufin. Finally we applied the fabricated OPD to the determination of IgA by fluorometric immunoassay on a microfluidic microchannel.

2. Experimental

2.1. Material and reagents

For the fabrication of the OPD, a PcCu(II) complex, obtained from Tokyo Kasei Co., Ltd., (Tokyo, Japan), was purified by three sublimations and was used as a p-type semiconductive material. Fullerene (C_{60}), with a purity of 99.95%, was obtained from Material Technologies Research Ltd., (OH, USA) and was used as received as an n-type semiconductive material. 2,9-Dimethyl-4,7-diphenyl-1,10-phenanthoroline (BCP) (Tokyo Kasei Co., Ltd., Tokyo, Japan) was used as a hole blocking material. An indium doped thin oxide (ITO) deposited glass plate (thickness of the ITO layer, 100 nm) was purchased from Sanyo Vacuum Industries Co., Ltd. (Osaka, Japan).

To evaluate the performance of the OPD as an optical detector, chemilumniescence from the reaction of luminol with horseradish peroxidase (HRP, IBU number: EC1.11.1.7, source: horseradish) in the presence of H_2O_2 was utilized. Luminol, H_2O_2 and HRP were obtained from Wako Chemical Co., Ltd., (Osaka, Japan). Resorufin, purchased from Aldrich–Sigma Inc., (USA), was used to evaluate the performance of the OPD for fluorescence detection.

For the fluorometric immunoassay for IgA, 10-acetyl-3,7-dihydoxyphenoxazine (Amplex Red) was purchased from Fluka (Buchs, Switzerland) and was used as a substrate for horseradish peroxidase (HRP). Human IgA, an anti-human IgA antibody (Goat, Poly) and an HRP labeled anti-human IgA (Goat, Poly) were purchased from Bethyl Laboratories, Inc. (TX, USA) as an ELISA kit for IgA. Bovine serum albumin (BSA) and an immune-enhancer were purchased from Wako Chemical Co., Ltd., (Osaka, Japan) as a blocking reagent at the wall surface of a microchip. All other reagents were analytical grade. All buffer solutions were prepared with deionized water purified on a Milli-Q System (Millipore Co., MA, USA) and sterilized by autoclaving (KS-243, Tomy Seiko Co., Ltd., Tokyo, Japan).

2.2. Preparation of organic thin film photodiode (OPD)

A strip-patterned indium doped tin oxide (ITO) layer, deposited on a glass slide, was prepared by a conventional photolithographic method. A photomask of 4 stripes (width 2 mm, length 20 mm) prepared by an ink jet printing technique on a polyester sheet (overhead projector sheet) was placed on the surface of the ITO layer deposited glass slide (25 mm × 25 mm × 0.7 mm^t), where a positive photo-resist had been coated, and was then irradiated with UV-light. The resulting slide glass was immersed in an aqua regia solution to etch the un-irradiated part of the ITO. The resist on the glass slide was dissolved in a developing solution, resulting in the formation of stripe-patterned ITO deposited glass slide. After cleaning the resulting glass by sonication in acetone, it was dried in a stream of nitrogen gas and was placed into an ozone cleaner (UV253, Filgen Inc., Tokyo, Japan). A PcCu(II) layer, a carbon 60 (C_{60}) layer and bathocuproine (BCP) layer were prepared on the ITO deposited slide glass by a vapor deposition method through a stainless steel mask with a 20 mm × 20 mm opening in the chamber for depositing organic material for a vacuum evaporation system (E-110, ALS Technology, Kanagawa, Japan). The thickness of the PcCu(II), C_{60} and BCP were 57 nm, 35 nm and 10 nm respectively, which were controlled by adjusting the time and deposition rate (0.03–0.05 nm/s, under ca 1×10^{-3} Pa), which was monitored by means of a quartz microbalance. The resulting organic layer deposited slid glass was subsequently transferred to the next chamber for depositing the inorganic material and a 50 nm thick silver layer was prepared on the organic layered slide glass using a stainless steel mask with a 2 mm × 20 mm opening perpendicular to the stripe of ITO layer. Finally the fabricated OPD substrate was bonded to a glass substrate for sealing by using a UV hardening resin in a glove box (KK-011 AS-Extra, ALS Technology, Kanagawa, Japan).

2.3. Measurement of current–voltage characteristic (JV curve) and incident photon-to-current conversion efficiency (IPCE) of OPD

The resulting OPD was placed on a solar illumination stage and current–voltage curves (*JV* curves) in the dark and under simulated AM 1.5 solar illumination (Otento-Sun II, KP type, Bunkokeik, Japan) with a Xe-lamp (Model XCS-150 A, Jasco, Japan) were obtained via the use of a source meter (R6423, Advantest, Japan). The IPCE was

calculated from the photocurrent, which was measured using a source meter under irradiation from a monochromatic light source (SK-U1152X, Ushio Inc., Japan) and a monochrometer (SM-10P, Bunkokeiki, Japan) from 400 nm to 800 nm at intervals of 10 nm. The incident light power of the monochromatic light was calibrated using a Si photodiode (BS-520, Bunkokeiki, Japan) for calculating the conversion efficiency of the OPD.

2.4. Evaluation of photosensitivity of OPD as a photodetector

In order to evaluate the photosensitivity of the OPD, a conventional LED (maximum wavelength 493 nm or 592) was fixed at one end of a cylindrical hole (diameter: 5 mm Ø) prepared using a stack of black acrylic resin plates (thickness of one plate: 1.0 cm) and the OPD was placed at the other end of the cylindrical opening. The photocurrent of the OPD for light from the LED was measured using a picoammeter (6485, Keithley Instruments, Inc., OH, USA). In this case, in order to change the light intensity by varying the distance between the OPD and the LED, the number of plates in the stack of black acrylic resin plates was increased. The distance between the OPD and the LED could be changed from 2.0 cm to 10.0 cm. For calibration of the intensity of light from the LED, a power meter consisting of a Si photodiode (1918-C, Newport Co., CA, USA) was placed at the end of the cylindrical hole at the same distance of the stack of the black acrylic resin plate instead of the OPD.

2.5. Preparation of microchip

The PDMS microchip with a modified Y type microchannel (two inlets and one outlet) was prepared on the PDMS coated glass substrate ($60\,mm \times 40\,mm \times 2\,mm^t$) using a photolithographic method. The width and the length of the main straight channel were 2 mm and 40 mm, respectively. Another inlet channel with a width of 1 mm and a length of 10 mm was merged with the main channel at right angles, at a distance of 20 mm from the inlet of the main channel. The preparation procedures were as follows. A portion of 1.5 mL of SU-8 was spin-coated (500 rpm for 20 s and then 2000 rpm for 20 s) on the glass substrate using a spin coater (1H-DX, Mikasa Co., Ltd., Tokyo, Japan) and the resulting substrate was then heated on a hot plate (ND-1, As One, Osaka, Japan) at 95 °C for 10 min. An OHP sheet printed with the flow pattern with a modified Y type was placed on the SU-8 coated substrate and the sample irradiated with a UV light for 30 s using an exposure box (BOX-W9B, Sunhayato, Tokyo, Japan). The resulting substrate was heated again at 60 °C for 1 min and 95 °C for an additional 5 min on the hot plate. The substrate was immersed in a SU-8 Developer solution for about 2 min and washed with isopropyl alcohol and then baked at 200 °C for 3 min on a hot plate. Thus, the master template of the microchip, with the channel part intact, was prepared. The thickness of the SU-8 layer on the substrate was ca 100 μm.

A mixture of a PDMS prepolymer and a curing reagent at a weight ratio of 10:1 was degassed in a vacuum and about 4 g of the mixture was poured onto the master template, which was surrounded by a wall of Scotch tape, and the resulting master template was heated at 60 °C for 30 min to form the channel. At the same time, the PDMS coated glass substrate was prepared by spin-coating the PDMS prepolymer onto the glass substrate at a rotation speed of 1000 rpm. After curing at 60 °C, the PDMS mold was detached from the master template and two inlet holes and one outlet hole (diameter 1.5 mm Ø) were drilled at the end of the channel of the PDMS mold using a punch. The PDMS mold and the PDMS coated glass substrate were exposed to an oxygen plasma for 30 s using a plasma generator (BD-20AC, Electro-Technic Products Inc., IL, USA) and the 2 objects were then attached to each other immediately. The resulting microchip was held at 120 °C for 4 h in an oven to complete adhesion of the two parts. Finally PEEK tubes (0.125 mm i.d., 1/16 in. o.d. 50 mm long) were mounted at the inlets and outlet of the microchip with an adhesive (Epoclear, Konishi Co., Japan). Thus the microchip shown in Fig. 1, which was equipped with a main microchannel (2 mm in width, 40 mm in length and 100 μm in depth) and a branched microchannel (1 mm in width 15 mm in length and 100 μm in depth), was fabricated.

2.6. Fluorescence detection system

Fig. 1 shows a schematic flow diagram for fluorescence detection system using the OPD as an optical detector. The system consisted of two syringe pumps (NE-1002X, New Era Pump Systems Inc., NY, USA), two injectors (9725, Rheodyne, CA, USA), the prepared PDMS microchip, a band pass filter (ET620/60 nm, Chroma Technology Co., VT, USA), the developed OPD and a LED light source (LLS-505, KLV Co., Tokyo, Japan), a picoammeter. For the fluorometric determination of resorufin, syringe pump 1 and injector 1 were used but syringe pump 2 and injector 2 were not. A 0.1 M phosphate buffer (pH 7.4) solution was used as a carrier solution and was pumped using syringe pump 1 at the flow rate of 20 μL/min and resorufin solutions at the different concentrations (0.5–50 μM) were injected from the sample injector 1 with a 50 μL loop. The excitation light from the LED was directed to the microchip at the position 30 mm from the inlet of the microchannel using an optical quartz fiber (core diameter: 600 μm, Ocean Optics Inc., USA). The fabricated OPD was placed on an X–Y stage and was placed above the microchip through the band pass filter. The sensing part of the OPD (2 mm × 2 mm) was adjusted so as to permit the fluorescence to be detected sensitively, where the excitation light was irradiated on the bottom side of the microchip. A photocurrent from the OPD was measured with the picoammeter, and the obtained data were transferred to a personal computer through a GPIB interface (KUSB-488A, Keithley Co., USA).

2.7. Immunoassay for IgA

The flow system shown in Fig. 1 was used for the fluorometric immunoassay for IgA. The carrier solution in syringe 1 and 2 both contained a 50 mM Tris–HCl buffer solution (pH 8.0) containing 0.14 M NaCl and a separate flow rate of 20 μL/min, depending on the immunoassay protocol. The scheme for the sandwich immunoassay is shown in Fig. 2. A 20 μL aliquot of a 1 M NaOH solution and a 1 M HCl solution was injected from the injector into the carrier stream at 5 min intervals to wash the inside of the tube and the microchannel. In order to immobilize the primary anti-IgA antibody on the surface of the microchannel, 20 μL of a 200 μg/mL anti-human IgA antibody was injected into the carrier stream from injector 1 and after 60 s, syringe pump 1 was stopped for 2 h to maintain the antibody solution in the microchip. Syringe pump 1 was re-started and the carrier solution allowed to flow for 10 min, to wash out the antibody solution from the microchannel. A 20 μL aliquot of a 10 mg/mL BSA solution prepared using the same 50 mM Tris–HCl buffer solution as the carrier solution was injected from injector 1 into the carrier stream and after 60 s, syringe pump 1 was stopped for 60 min, to allow BSA to block the surface of the microchip. Syringe pump 1 was then re-started and the carrier solution allowed to flow for 10 min, to wash out the BSA solution. A 20 μL aliquot of several concentrations of a human IgA solution (15 ng/mL–1 μg/mL) containing 10 mg/mL BSA was injected from injector 1 into the carrier stream and the carrier solution allowed to flow for 5 min. In order to avoid contamination, a 20 μL aliquot of 5 μg/mL HRP-labeled anti-human IgA antibody (2nd antibody) solution containing 10 mg/mL BSA was injected from injector 2 into the carrier stream driven by syringe pump 2 at a flow rate of 20 μL/min for 5 min. During this period, pump 1 was stopped. In order to reduce the non-specific adsorption of the 2nd antibody, a 20 μL aliquot of the phosphate buffer solution

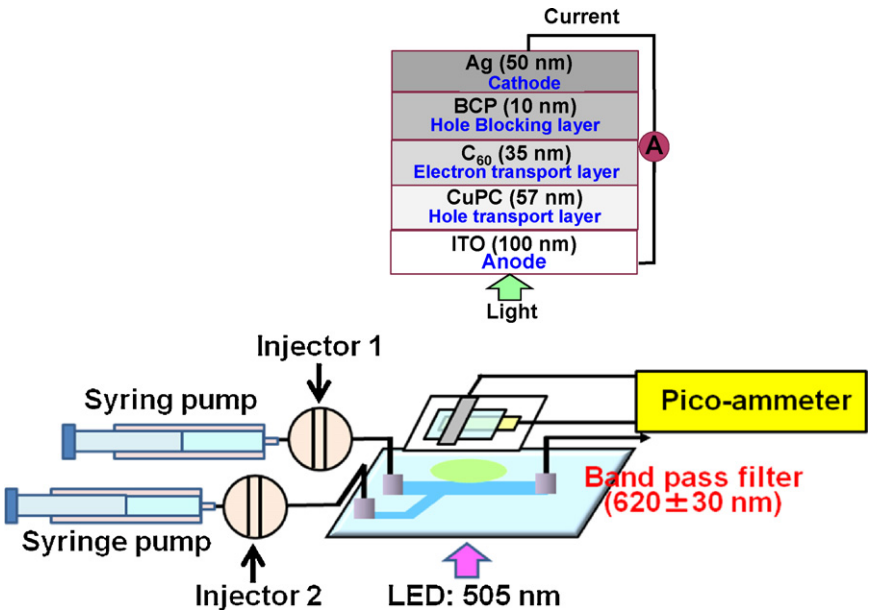

Fig. 1. Structure of the OPD and a schematic flow diagram of the fluorescence detection system constructed from two syringe pumps, two injectors, the PDMS microchip, a band pass filter, and commercial LED, the OPD fabricated in this work and a pico-ammeter.

(pH 7.4) containing 10 mg/mL BSA and 0.5% Tween-20 was injected from injector 1 into the carrier stream for 5 min. Finally a 50 μL aliquot of 0.1 mM Amplex Red containing 1 mM H_2O_2 was injected from injector 1 and the carrier allowed to flow for 5 min. The fluorescence due to resorufin, generated from the enzymatic reaction of HRP with Amplex Red, was measured using the fabricated OPD and the signal was obtained as a photocurrent signal. After measuring the fluorescence intensity, a 20 μL aliquot of a 0.1 M glycine–HCl buffer (pH 2) was injected from injector 1 into the carrier stream to dissociate the sandwich immunocomplex that had been initially formed on the microchip, when the first antibody was immobilized on the microchip. These processes were repeated starting with the injection of the sample solution containing human IgA at different concentrations.

3. Results and discussion

3.1. Fundamental performance of OPD

3.1.1. JV characteristics of OPD

Fig. 3(a) and (b) shows current–voltage curves (*JV* curves) for the OPD obtained by scanning the applied potential between the silver cathode and the ITO anode under illumination by quasi-sun light at an air mass of 1.5 (AM 1.5) and under dark conditions, respectively, as described in Section 2.3. As shown in Fig. 3(b), no photocurrent was detected under dark conditions up to ca +0.2 V and the current flow at a higher applied potential than +0.2 V, indicating a functional p–n junction between the C_{60} and PcCu(II) layers. While the photocurrent was observed under illumination by quasi-sun light, about 3 mA cm^{-2} was observed without an applied potential, indicating that the prepared OPD showed sufficient sensitivity to visible light. From the *JV* curve shown in Fig. 3(a), the open-circuit voltage, Voc, short-circuit current density, Jsc were calculated to be 0.49 V and −3.1 mA cm^{-2}, respectively. The open-circuit current density, Jop, and the open-circuit potential, Vop, at which maximum power is provided, were −2.3 mA and 0.33 V, respectively. The fill factor, F.F, and the energy conversion efficiency, η (%), respectively defined by Eqs. (1) and (2) were calculated to be 0.50 and 0.75%, respectively.

$$\text{Fill factor(F.F)} = \frac{(\text{Vop} \times \text{Jop})}{(\text{Voc} \times \text{Jsc})} \quad (1)$$

$$\eta = (\text{Voc} \times J) \times \text{F.F} \times \frac{100}{\text{Pi}} \quad (2)$$

where, Pi is the energy density of incident light. In this experiment, from the light source used, Pi is 0.1 W/m^2.

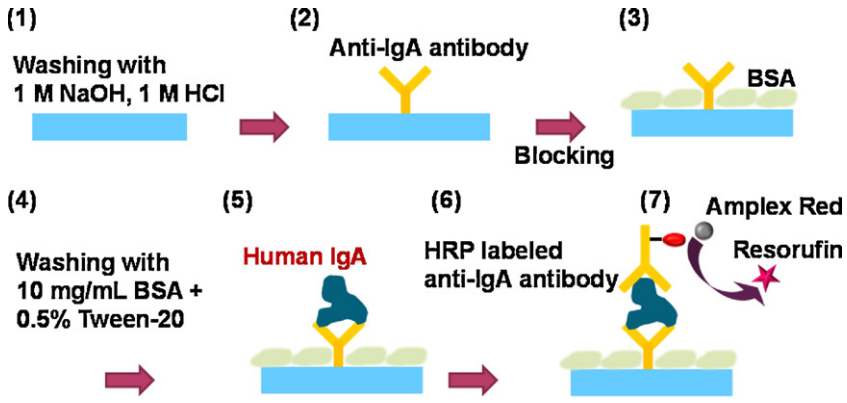

Fig. 2. Scheme showing the protocol for the sandwich immunoassay.

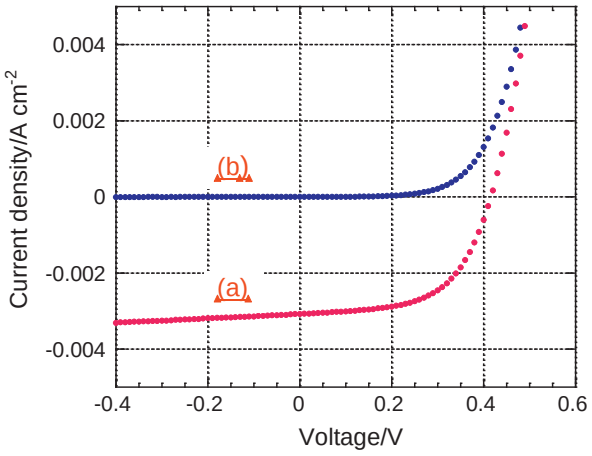

Fig. 3. *JV* curves for the OPD. (a) Under irradiation by quasi-solar light, (b) under dark conditions.

The characteristics of the present OPD, composed of C_{60} and PcCu(II) layers, is similar to that reported in previous paper [21].

3.1.2. Incident photon to current conversion efficiency

Fig. 4 shows the incident photon-to-current conversion efficiency (IPCE), defined as the ratio of the current flowing in the out-side circuit to the number of photons irradiated to the surface of the OPD, as a function of the wavelength, where the incident light was monochronized by the monochrometer. Its power was initially calibrated using the Si photodiode, as described in Section 2. As can be seen from Fig. 4, more than 20% of IPCE is achieved by the present OPD and a peak maximum around 430 nm and double peaks around 620 and 700 nm are observed. The ICPE for the OPD is known to be governed by several efficiencies such as exiton generation, approaching of exitons to the p–n junction interface, charge separation at the interface between holes and electrons and the transport of holes and electrons, respectively, to an anode and a cathode. Since the diffusion length of the exiton is in the order of several nanometers, the charge carrier generated at the p–n junction interface is thought to affect the IPCE. Therefore the absorbance efficiency of the organic layers of the OPD contributes to the ICPE. The peak maximum at around 430 nm is due to the absorbance band of the C_{60} and that at around 620–700 nm arises from the absorbance bands for the PcCu(II) complex. The present OPD shows good sensitivity for the detection of light for chemiluminescence

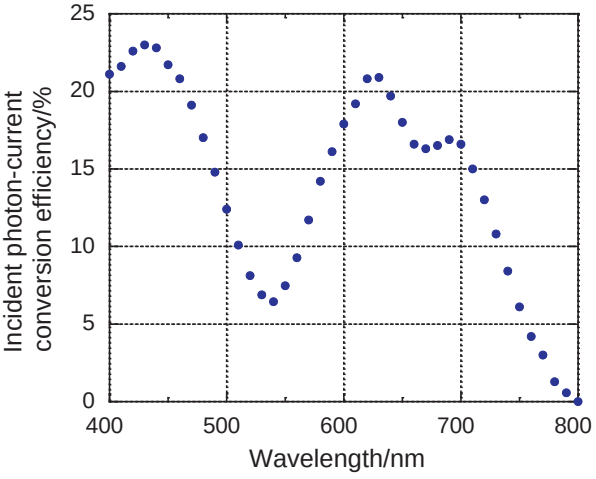

Fig. 4. Relationship between incident photon-to-current conversion efficiency (IPCE) and the wavelength of irradiated light.

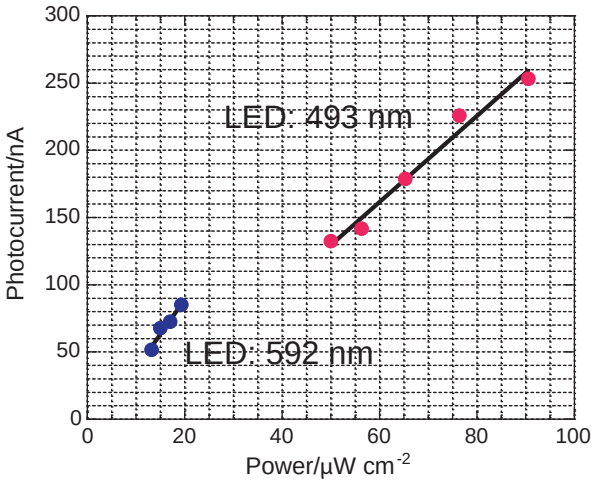

Fig. 5. Relationship between the photocurrent of the present OPD and LED power measured by a power meter based on a silicon diode. The LEDs used for the light sources have peak maxima of 493 nm (green) and 592 nm (yellow).

from luminol as well as fluorescence from resorufin. Hofmann et al. have been prepared a similar OPD constructed from PcCu(II) complex and C_{60} and measured the external quantum efficiency. The maximum external quantum efficiency of about 30% was obtained between 600 and 700 nm, however in the range from 400 to 500 nm, the quantum efficiency was about 10%, which is lower than that obtained in the present OPD. This may be due to the fact that the relative thickness of the C_{60} layer of the present OPD is thicker than that of the OPD prepared by Hofmann et al.

3.1.3. Photosensitivity of OPD

In order to evaluate the photosensitivity of the fabricated OPD, two visible lights with maximum intensities at 493 nm and 592 nm were used as model lights for the chemiluminescence of luminol (ca 470 nm) and the fluorescence of resorufin (590 nm). Fig. 5 shows the relationship between the photocurrent observed by the OPD and the power of the light, as observed by the power meter when the two LED lights were irradiated through the cylindrical hole at several different distances from the OPD and the power meter. In this case, the area of the OPD is 4×10^{-2} cm^2. As can be seen from Fig. 5, a good linear relationship exists between the two observed values. This indicates that the photosensitivity of the present OPD is linear with respect to the light intensity at a certain wavelength. The slope of the line is an indicator of the performance of the photodetector, the sensitivity in the A/W unit. The sensitivity of the OPD for 493 nm and 592 nm light was calculated to be 0.07 A/W and 0.11 A/W, respectively. The difference in responsivity to each irradiated light with different wavelengths may be due to differences in the IPCEs, because the IPCEs for the present OPD at wavelengths of around 490 nm and 590 nm are not much different, at ca 15% and ca 17%, respectively. Moreover, the sensitivity difference due to the wavelength dependency of the power meter is nearly compensated by a filter of the original product. The photoresponsivity of the present OPD at 590 nm (0.11 A/W) is about a half of that obtained by an OPD prepared from P3HT/PCBM, 0.25 A/W at 550 nm [19].

3.1.4. Performance of OPD in chemiluminescence detection

Prior to utilizing the OPD for measuring the fluorometry of resorufin and in a fluorometric immunoassay for IgA on a microchip, the OPD was evaluated for the detection of chemiluminescence light generated from the reaction of luminol with HRP in the presence of H_2O_2. A 1.5 mL aliquot of a 50 ppm HRP solution was quickly added to a quartz cell (10 mm path length) that contained a 1.5 mL aliquot of a 100 μM luminol solution containing

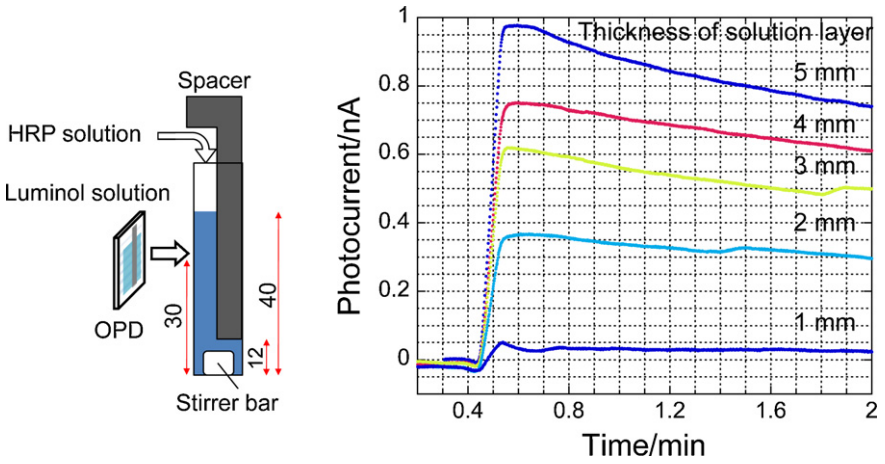

Fig. 6. Detection of chemiluminescence generated from the reaction of HRP with luminol in the presence of H_2O_2 at thickness of the solution layer. The thickness of the solution layer was changed by inserting the black colored spacer into the 10 mm path length quarts cell.

5.0 mM H_2O_2 and 300 μM *p*-iodophenol. Chemiluminescence light was measured by the OPD, which was attached to the side wall of the quartz cell, as shown in Fig. 6(a). The solution in the quartz cell was magnetically stirred with a stirring bar during the measurements. A plot of the photocurrent against time obtained by the OPD for the generation of chemilumnescence is shown in Fig. 6(b). In this case the thickness of the solution layer was changed from 1 mm to 5 mm by inserting the black colored spacer with the thickness of 9–5 mm into the quartz cell. The chemiluminescent signal increased steeply within several seconds and gradually decreased with time. The maximum wavelength of the chemiluminescence from the luminol reaction is known to be around 470 nm, which is one of the maximum IPCE of the present OPD, as shown in Fig. 4. The data shown in Fig. 6(b) indicates that the OPD shows a good sensitivity for detecting the chemiluminescence, depending on the thickness of the solution where the chemiluminescence light is emitted. The photocurrent of a level of approximately 0.1 nA could be measured by the present OPD. The measured powers (using a power meter) of the present chemiluminescence were around 0.1–0.3 μW/cm^2 and the photocurrent obtained by the OPD were in good agreement with the responsivity, as obtained by the commercial LED with an emission wavelength of 493 nm, as shown in Fig. 5.

3.2. Fluorometry of resorufin on a microchip using OPD as an optical detector

In the present fluorescence detection by the OPD, a parallel optical arrangement was utilized for excitation light source and fluorescence light detection, largely because of the ease of the setup. The excitation light from the LED was irradiated from the beneath the microchip via an optical fiber with a 600 μm core diameter and the OPD was located above the microchip at the same position as the optical fiber through the band pass filter. Since the present OPD show a wide range of sensitivity, as shown in Fig. 4, the background signal from the excitation light interfered with the fluorescence detection with the OPD, the use of a band pass filter was found to be necessary for the present optical arrangement. In spite of using a band pass filter, a background current of about 0.4 nA was observed, due to the excitation light.

The performance of the OPD for fluorescence detection was evaluated using resorufin as a model compound and also an enzymatic product of Amplex Red for an immunoassay of IgA. A 50 μL aliquot of different concentrations of a resorufin solution was injected into the phosphate buffer carrier solution at the flow rate of 20 μL/min. Fig. 7(a) shows the time course for the photocurrent as a fluorescence signal obtained by the OPD. Trapezoid-shaped signals were obtained for the resorufin samples, since the injection volume was sufficiently large, compared with the cell volume of the present microchip. This is due to the negligibly small dispersion of the sample solution in the microchip. A significant signal was observed for the resorufin solution at concentrations higher than 5 μM by the present OPD detector. An average of the photocurrent at the plateau of the signal (the period between 80 s and 150 s) was plotted against the concentration of resorufin and the data are shown in Fig. 7(b). A linear relationship between the concentration of resorufin and the photocurrent was found, with a correlation coefficient of 0.993. The detection limit defined as the signal to noise ratio of 3, where noise level of the present optical system for flowing the carrier solution was 0.03 nA, was calculated to be 1 μM from the calibration line shown in Fig. 7(b). The fluctuation of fluorescence signals and background signals, which are due to the fluctuation of the excitation light were both small, at about 0.03 nA. This indicates that the fluctuation of the sensitivity of the OPD is sufficient for detecting a low intensity of fluorescence light.

3.3. Fluorometric immunoassay for IgA on a microchip by using OPD as optical detector

Fig. 8 shows the time-course for the photocurrent of the OPD when the Amplex Red solution was finally introduced into the chip, where the sandwich immunocomplex formed by the previous two step immunoreactions was located ((7) in Fig. 2). In this case, since the volume of the Amplex Red solution was 50 μL, similar trapezoid-shaped signals were observed, the same as for the detection of resorufin described in Section 3.2. However the difference from the case of Section 3.2 is that in this case, the enzyme reaction proceeded simultaneously during the detection of fluorescence from resorufin. Since the volume of the microchannel is ca 6 μL and the flow rate of the Amplex Red solution was 20 μL/min, the average residence time (reaction time) for Amplex Red with HRP on the secondary antibody was calculated to be less than 20 s. Therefore the resorufin produced during the 20 s it was in contact with the Amplex Red solution with the HRP-labeled secondary antibody on the microchip can easily be observed by the OPD. Also since the volume of the injected Amplex Red solution was 50 μL, the fluorescence signal is calculated to continue for at least for 2.5 min. This estimation is reasonable, based on the plateau region shown in Fig. 8. In this case noise derived from the photocurrent is relatively larger than that of the photocurrent measured for resorufin directly. This may be due to an overlapped fluctuation of the enzymatic reaction on the surface of the microchannel. The average of

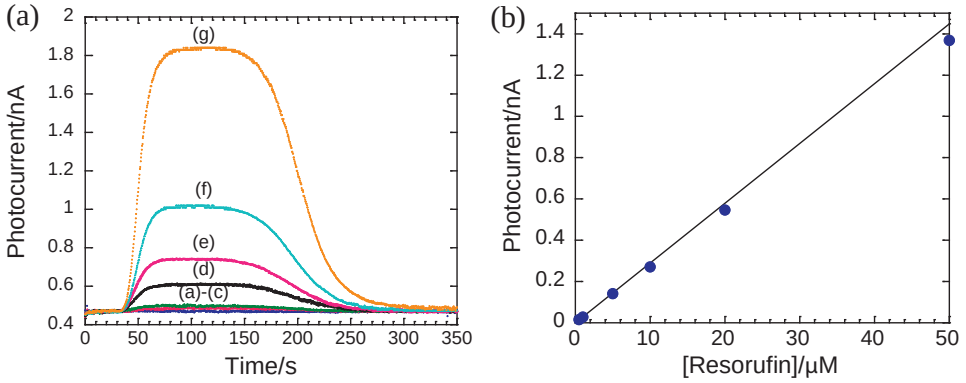

Fig. 7. Fluorescence response of OPD for resorufin (a) and a calibration curve for resorufin based on the change in fluorescence intensity from the baseline to the plateau region of the response curve (b). Concentration of resorufin injected into the carrier stream: (a) 0, (b) 0.5, (c) 1.0, (d) 5.0, (e) 10, (f) 20, (g) 50 μM. Baseline fluctuation of photo current was within 0.03 nA.

the photocurrent at the plateau of the signal (the period between 80 s and 150 s) was plotted against the concentration of IgA solution (Fig. 8(b)), which was introduced into the microchip at the second step of the immunoassay ((5) in Fig. 2). In the concentration range up to 120 ng/mL, a good linear relationship between the photocurrent and the concentration of IgA was found observed and, at higher concentrations than 120 ng/mL, the photocurrent gradually increased with the concentration of IgA, as shown in Fig. 8(b). In the present immunoassay, after immobilization of the primary anti-IgA antibody on the PDMS microchip, the chip was able to use more than 10 times by regeneration of the chip by introducing the dissociation solution (0.1 M glycine–HCl buffer (pH 2)), as described in Section 2.7. Therefore the immobilization step, which required for 2 h in this case, can be omitted after the first measurements for the subsequent assays. The reproducibility experiments have been performed for the determination of the sample of 250 ng/mL IgA by 10 times repeated assays. As a result, the standard relative deviation of 21% was obtained and this value is almost the same as that obtained for the immunoassay using LED-induce fluorescence device by our previous paper [28]. In the present sandwich

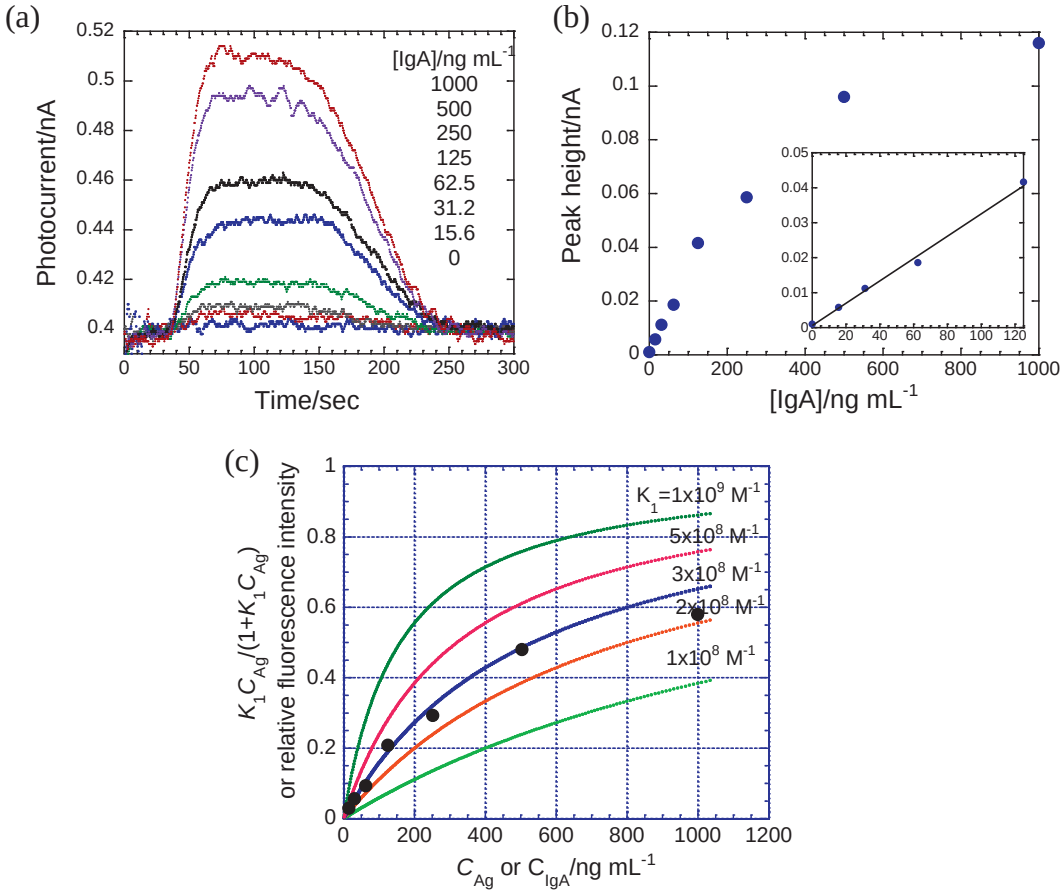

Fig. 8. Immunoassay of IgA using the OPD as an optical detector for fluorescence. (a) Fluorescence response of OPD as photocurrent, when the Amplex Red solution was introduced into the microchip, where the sandwich immunoreaction was carried out. (b) Calibration curve for IgA by plotting the photocurrent of OPD, which is the average for the time period from 70 s to 120 s in the plateau region of the response signal, against the concentration of IgA. (c) The simulated calibration curve for IgA based on Eq. (4) (see supporting information for simulation procedures).

immunoassay for IgA, the surface concentration of IgA bound to the primary antibody (abbreviated as Ab_1–Ag) is theoretically derived as follows by assuming a Langmuir-type adsorption isotherm equilibrium (details are shown in supporting information in this paper).

$$\frac{[Ab_1 - Ag]}{[Ab_1]^T} = \frac{K_1 C_{Ag}}{(1 + K_1 C_{Ag})} \quad (3)$$

where $[Ab_1–Ag]$ and $[Ab_1]^T$ are the surface concentration of the Ab_1–Ag complex and the total surface concentration of the primary antibody immobilized on the chip in the first step of the immunoassay ((2) in Fig. 2), respectively. K_1 and C_{Ag} are the binding constants for Ab_1 to the Ag and the concentration of Ag in the sample solution, respectively. In practice, a constant and large excess of the second antibody is introduced into the chip to complete the Ab_1–Ag complex on the surface of the chip to convert to a sandwich complex, Ab_1–Ag–Ab_2 ((6) in Fig. 2). Therefore, the surface concentration of the Ab_1–Ag complex formed at the second step can be assumed to be the same concentration as the sandwich complex, Ab_1–Ag–Ab_2, which is formed at the third step. Therefore at step (7) in Fig. 2, where the Amplex Red solution is introduced into the chip, the observed fluorescence intensity due to resorufin, which is the enzymatic product of the reaction of HRP on the secondary antibody with Amplex Red, is proportional to the surface concentration of the Ab_1–Ag–Ab_2 sandwiched complex on the chip. This indicates that the change in fluorescence intensity is related to the concentration of Ag through Eq. (3). Replacement of the numerator on the left hand side of Eq. (3) with the fluorescence intensity gives a relationship between the change in fluorescence intensity, ΔI, and the concentration of the Ag (Eq. (4)).

$$\Delta I \propto \frac{K_1 C_{Ag}}{(1 + K_1 C_{Ag})} \quad (4)$$

Fig. 8(c) shows the calculated curves for Eq. (4) as a parameter of the binding constant, K_1, and the observed data are plotted in this figure by appropriately scaling the photocurrent. When the fluorescence intensity change observed as the photocurrent for the present immunoassay for IgA is fitted to the calculated curves based on Eq. (4), $3 \times 10^8\ M^{-1}$ is the best fit for the binding constant, K_1. This value appears to be reasonable, compared with binding constants reported for several antibodies with antigen pairs [22–27].

4. Conclusion

A fluorometric flow-immunoassay for IgA using an OPD as an optical detector was developed. The OPD detector, comprised of a hetero-junction of C_{60} and PcCu(II) layers, was fabricated by a vapor deposition method. The OPD showed good sensitivity to visible light from 400 nm to 800 nm and a relatively higher sensitivity to light at 430 nm, 620 nm and 690 nm, which corresponds to the absorption band for the materials contained by the OPD. The chemiluminescence light from the luminol–HRP–H_2O_2 system can be detected by the OPD at levels as low as 0.1 $\mu W/cm^2$. The OPD was successfully applied to a flow-immunoassay for IgA, a marker of human stress, where a sandwich immunoassay was carried out on a microchip and the fluorescence form resorufin produced by an enzymatic reaction was detected. The detection limits for resorufin and IgA were determined to be 5.0 μM and 16 ng/mL, respectively. The fabricated OPD showed almost the same performance at least for one year. We are currently attempting to fabricate an optical sensing system combined with both the OPD with an organic light emitting diode on a microchip.

Acknowledgment

This work was supported in part by the Funding Program for World-Leading Innovative R&D on Science and Technology (FIRST).

Appendix A. Supplementary data

Supplementary data associated with this article can be found, in the online version, at doi:10.1016/j.talanta.2012.02.006.

References

[1] A. Manz, N. Graber, H.M. Widmer, Sens. Actuators B 1 (1990) 244–248.
[2] A. Rios, A. Escarpa, M.C. Gonzalez, A. Crevillen, Trends Anal. Chem. 25 (2006) 467–479.
[3] T. Vilkner, D. Janasek, A. Manz, Anal. Chem. 76 (2004) 3373–3386.
[4] Y.L. Yu, Y. Jiang, M.L. Chen, J.H. Wang, Trends Anal. Chem. 30 (2010) 1649–1658.
[5] S. Armenta, S. Garogies, M. de la Guardia, Trends Anal. Chem. 27 (2008) 497–511.
[6] M. Tokeshi, T. Minagawa, T. Kitamori, J. Chromatogr. A 894 (2000) 19–23.
[7] H. Nakajima, K. Kawata, H. Shen, T. Nakagama, K. Uchiyama, Anal. Sci. 21 (2006) 67–71.
[8] K. Sato, M. Tokeshi, H. Kimura, T. Ooi, M. Nakao, T. Kitamori, Anal. Chem. 72 (2000) 1144–1147.
[9] C. Ericson, J. Holm, T. Ericson, S. Hjerten, Anal. Chem. 72 (2000) 81–87.
[10] T. Masadome, K. Nakaumra, D. Iijima, O. Horiuchi, B. Tossanitada, S. Wakida, T. Imato, Anal. Sci. 26 (2010) 417–423.
[11] M. Tokeshi, M. Uchida, A. Hibara, T. Sawada, T. Kitamori, Anal. Chem. 73 (2001) 2112–2116.
[12] M.L. Chabinyc, D.T. Chiu, J.C. McDonald, A.D. Stroock, J.F. Christian, A.M. Karger, G.M. Whiteside, Anal. Chem. 73 (2001) 4491–4498.
[13] M. Hashimoto, K. Tsukagoshi, R. Nakajima, K. Kondo, A. Arai, J. Chromatogr. A 867 (2000) 271–279.
[14] J.B. Edel, N.P. Beard, O. Hofmann, J.C. de Mello, D.D.C. Bradley, A.J. de Mello, Lab Chip 4 (2004) 136–140.
[15] B. Yao, G. Luo, L. Wang, Y. Gao, G. Lei, K. Ren, L. Chen, Y. Wang, Y. Hu, Y. Qiu, Lab Chip 5 (2005) 1041–1047.
[16] K.S. Shin, Y.H. Kim, K.K. Paek, J.H. Park, E.G. Yang, T.S. Kim, J.Y. Kang, B.K. Ju, IEEE Electron Device Lett. 27 (2006) 746–748.
[17] Y.H. Kim, K.S. Shin, J.Y. Kang, E.G. Yang, K.K. Paek, D.S. Seo, B.K. Ju, J. Microelectromech. Syst. 15 (2006) 1152–1158.
[18] O. Hofmann, P. Miller, P. Sullivan, T.S. Jones, J.C. de Mello, D.D.C. Bradley, A.J. deMello, Sens. Actuators B 106 (2005) 878–884.
[19] X. Wang, M. Amatatongchai, D. Nacapricha, O. Hofmann, J.C. deMello, D.D.C. Bradley, A.J. deMello, Sens. Actuators B 116 (2009) 643–648.
[20] A. Pais, A. Banerjee, D. Klotzkin, I. Papautsky, Lab Chip 8 (2008) 794–800.
[21] N.S. Saricitfci, L. Smilowitz, A.J. Heeger, F. Wudl, Science 258 (1992) 1474–1476.
[22] N. Soh, T. Tokuda, T. Watanabe, K. Mishima, T. Imato, T. Masadome, Y. Asano, S. Okutani, O. Niwa, S. Brown, Talanta 60 (2003) 733–745.
[23] M. Kobayashi, M. Sato, Y. Li, N. Soh, K. Nakano, K. Toko, N. Miura, K. Matsumoto, A. Hemmi, Y. Asano, T. Imato, Talanta 68 (2005) 198–206.
[24] Y. Li, M. Kobayashi, K. Furui, N. Soh, K. Nakano, T. Imato, Anal. Chim. Acta 576 (2006) 77–83.
[25] Y. Li, J. Ren, H. Nakajima, N. Soh, K. Nakano, T. Imato, Anal. Sci. 23 (2007) 1–9.
[26] Y. Li, J. Ren, H. Nakajima, B.K. Kim, N. Soh, K. Nakano, T. Imato, Talanta 77 (2008) 473–478.
[27] M. Tanaka, K. Sakamoto, H. Nakajima, N. Soh, K. Nakano, T. Imato, Anal. Sci. 25 (2009) 999–1005.
[28] H. Nakajima, M. Yagi, Y. Kudo, T. Nakagama, T. Shimosaka, K. Uchuiyama, Talanta 70 (2006) 122–127.